

# Magnetorheological Finishing of IR Materials

## MRF of Optical Glasses

In magnetorheological finishing (MRF), a magnetic-field-stiffened ribbon of fluid is used to polish out a workpiece. Removal occurs through the shear stress created as the ribbon is dragged into the converging gap between the part and some reference or carrier surface. The zone of contact is restricted to a spot that is smaller than the part's diameter. The removal spot constitutes a subaperture lap that conforms perfectly to the local topography of the part. Deterministic finishing of flats, spheres, and aspheres is accomplished by mounting the part on a rotating spindle and sweeping it through the spot under computer control, such that dwell time determines the amount of material removed. The MR fluid lap is unique because (1) its compliance is adjustable through the magnetic field, (2) it carries heat and debris away from the polishing zone, (3) it does not load up, and (4) it does not lose its shape. A preliminary theory and an extensive review of the MRF process are given elsewhere.<sup>1,2</sup>

## 1. "Standard" MR Fluid

To date most MRF work has utilized an MR fluid consisting of magnetic particles of carbonyl iron (CI) in water, with small concentrations of stabilizers added to inhibit oxidation. Although this formulation will polish glass, removal rates are accelerated with the addition of cerium oxide ( $\text{CeO}_2$ ). A "standard" formulation used in many experiments at the University of Rochester's Center for Optics Manufacturing (COM) consists of (given in vol %) 36/CI, 6/ $\text{CeO}_2$ , 55/water, and 3/stabilizers. This high-solids-content fluid exhibits an apparent viscosity<sup>3</sup> of  $\sim 0.5 \text{ Pa}\cdot\text{s}$  outside of a magnetic field. In a magnetic field of 160 to 240 kA/m (2 to 3 kG), the apparent viscosity exceeds  $\sim 10,000 \text{ Pa}\cdot\text{s}$  at a shear rate of  $8/\text{s}$ ,<sup>4</sup> making it stiff enough to support loads for finishing. Figure 72.28 gives initial size histograms and median particle sizes for the solid particles.<sup>5</sup> The CI (left top) @  $4.5 \mu\text{m}$  is in the middle size range for commercially available magnetic powders,<sup>6</sup> whereas the  $\text{CeO}_2$  (left bottom) @  $3.5 \mu\text{m}$  is a coarse, impure, and aggres-

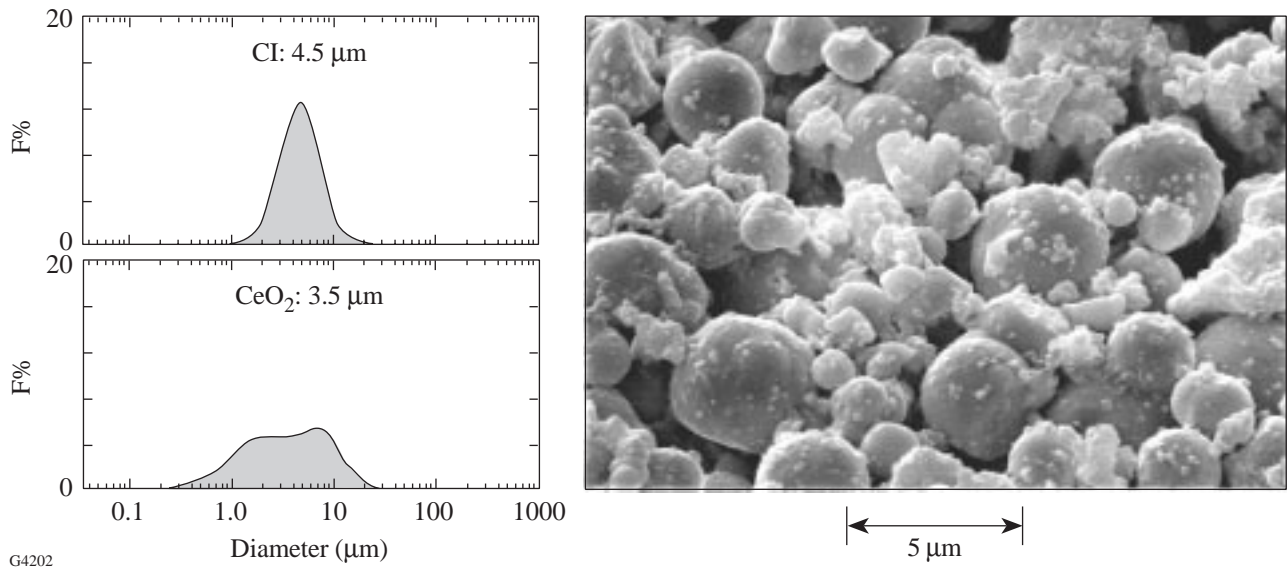


Figure 72.28  
Histograms showing initial particle sizes of solids in MR fluid. The SEM shows the solids after one week of use.

sive commercial polishing abrasive.<sup>7</sup> The scanning electron micrograph (SEM) of the MR fluid shown on the right in Fig. 72.28 was taken after one week of use. The round CI particles are essentially unaltered from their initial median particle size, but the irregularly shaped CeO<sub>2</sub> particles have been broken down to smaller sizes by constant milling action of the CI.

## 2. MRF Machine Platforms

In MRF, the workpiece is positioned above a moving surface that supports and carries a shaped ribbon of MR fluid into and through the polishing zone. The dc field from an electromagnet, located just below the carrier surface and centered under the workpiece, stiffens the ribbon before it contacts the part. Two machine configurations are shown in Fig. 72.29. The research testbed<sup>8</sup> in Fig. 72.29(a) consists of a 560-mm-diam rotating aluminum plate with a shallow trough along its rim. With this machine, it is possible to conduct screening experiments on different MR fluids and/or workpiece materials, provided that the test samples used are convex and less than 50 mm in diameter. Figure 72.29(b) shows the vertical wheel configuration used in the new prototype MRF machine.<sup>9</sup> Here, the wheel rim is a segment of a 150-mm-diam sphere. Convex, flat, or concave parts up to 100 mm in diameter can be finished without changing the setup.

## 3. Removal Rates, Polishing Spots, and Smoothing of Optical Glasses

Removal rates are obtained by generating spots as illustrated in Fig. 72.30. With the part mounted on a stationary (nonrotating) spindle, a program is used that moves the lens or surface to be polished into the field-stiffened ribbon at a fixed

contact angle of  $\sim 5^\circ$ . Material removal occurs during the 5- to 10-s contact time between ribbon and part. Peak and volumetric removal rates are calculated from interferometric data obtained on a phase-shifting interferometer<sup>10</sup> after correcting for the initial surface shape. It is important to measure removal rates for surfaces that are initially well polished out (rms surface roughness less than 5 to 10 nm). This avoids reporting erroneously high rates of removal that are seen for spots taken on ground surfaces. Usually, three spots are generated over several minutes, and the average result is reported. Data for fused silica suggest that results are good to  $\pm 4\%$ – $5\%$ .

The shape and magnitude of material removed in the polishing spot are used in two ways. Peak removal rates in  $\mu\text{m}/\text{min}$  give an indication of polishing efficiency for different materials when studied under identical fixed conditions. Volumetric removal rates are necessary for determining the machine program and finishing time required to process a specific part geometry.

By fixing all process parameters, it is possible to use MRF to study removal rates and conduct finishing experiments on a variety of optical glasses. Process conditions and experimental results are given in Table 72.IV, Fig. 72.31, and Fig. 72.32. The standard MR fluid is very effective at removing mass from silicates, borosilicates, lead silicates, lanthanum borates, and phosphates. Peak removal rates as high as 10 to 12  $\mu\text{m}/\text{min}$  are seen for soft glass compositions. Rates are between 1 and 2  $\mu\text{m}/\text{min}$  for the hardest glasses. An excellent positive linear correlation between volumetric removal rate and  $E^{5/4}/K_c H_k^2$  ( $E$ , Young's modulus;  $K_c$ , fracture toughness;  $H_k$ , Knoop hardness) is seen in Fig. 72.31.<sup>11</sup>

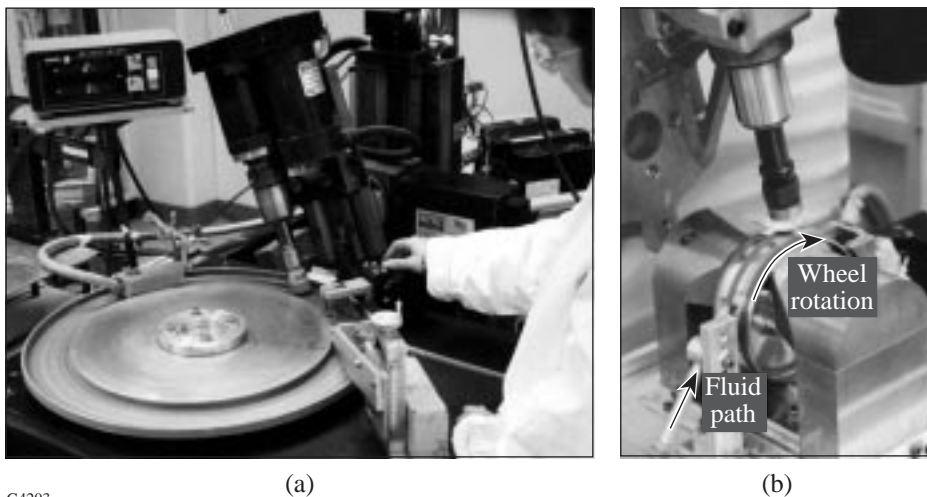


Figure 72.29  
(a) Horizontal-trough MRF machine;  
(b) vertical-wheel MRF machine.

G4203

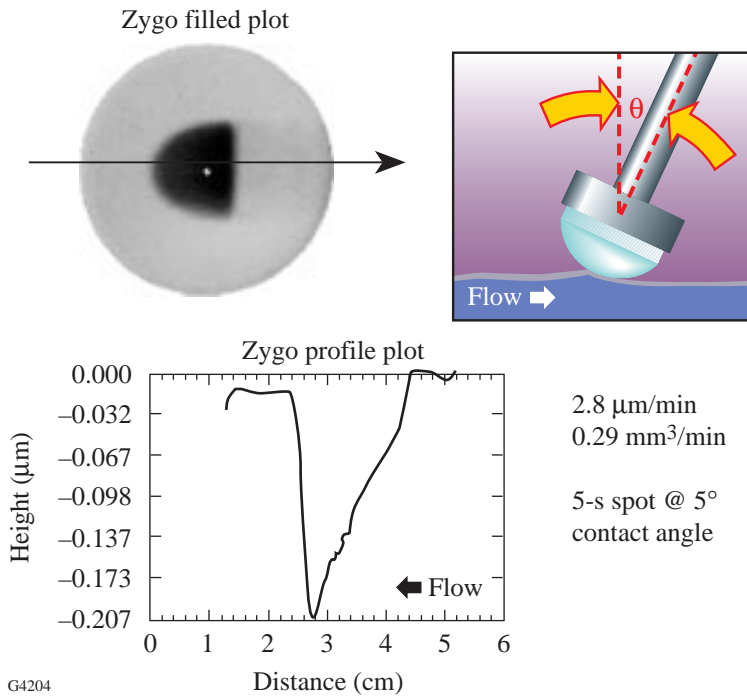


Figure 72.30  
Removal rates are derived from polishing spots. Interferometry is used to determine the peak and volumetric removal for a part that is positioned without spindle rotation in the MR fluid ribbon at a  $\sim 5^\circ$  angle for  $\sim 5$  s.

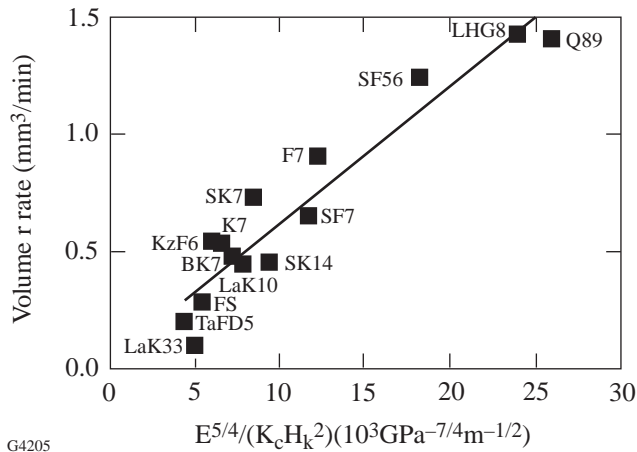


Figure 72.31  
Volumetric removal rates for optical glasses under fixed processing conditions given in Table 72.IV, plotted against a set of mechanical properties as described in the text.

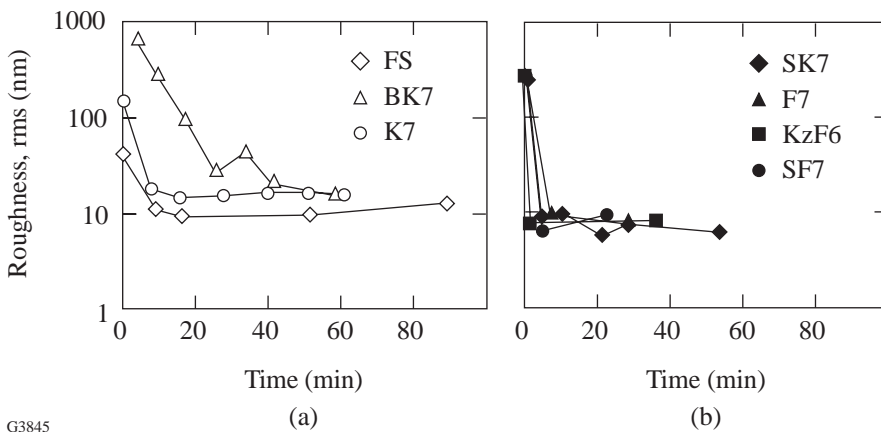


Figure 72.32  
Smoothing to remove microroughness<sup>12,13</sup> on glass surfaces under conditions given in Table 72.IV. Levels of  $\sim 1$  nm rms are achieved in 10 min with the “standard” MR fluid.

G4204

G4205

G3845

Table 72.IV: Removal-rate results with “standard” MR fluid on optical glasses.

Conditions:		
<ul style="list-style-type: none"> <li>• Plano-convex plugs, ~40-mm diam × 70-mm radius; pitch polished</li> <li>• Horizontal-trough machine</li> <li>• Trough velocity, 20 rpm (~0.5 m/s)</li> <li>• Work spindle fixed for spots, 70 rpm for polishing</li> <li>• Ribbon height/gap, 2/1 mm</li> <li>• Magnet current, 8 A</li> </ul>		
Glass <sup>(a)</sup>	Peak <i>r</i> rate μm/min	Vol. <i>r</i> rate mm <sup>3</sup> /min
KzF6 (S)	7.81	0.55
F7 (S)	11.85	0.91
LHG8 (H)	9.16	1.43
SF7 (S)	8.48	0.65
SF56 (S)	9.24	1.24
Q89 (K)	7.75	1.40
K7 (S)	4.87	0.53
FS (C, HA)	2.08	0.29
BK7 (S,O)	4.03	0.48
SK7 (S)	10.10	0.73
SK14 (S)	4.79	0.46
LaK10 (S)	2.42	0.45
LaK33 (S)	0.99	0.11
TaFD5 (H)	1.87	0.21

(a)(S) Shott, (H) Hoya, (K) Kigre, (C) Corning,  
(HA) Heraeus Amersil, (O) Ohara.

The ability of MRF to remove mass from a surface is necessary to eliminate subsurface damage and accomplish figure correction, but is not sufficient: MRF must also smooth away surface microroughness. This is done exceedingly well for glass. Figure 72.32 shows the evolution of surface microroughness with elapsed finishing time for fused silica and six optical glasses, measured with noncontacting optical profilometry.<sup>12,13</sup> Conditions are as indicated in Table 72.IV. The final rms surface microroughness, independent of glass type, is ~1 nm. The smoothing process is sensitive to the initial condition of the glass surface and the glass hardness. If the initial rms surface microroughness is less than ~30 nm, smoothing occurs in 5 to 10 min. More time is required for rougher surfaces (e.g., the result for BK7 in Fig. 72.32).

## MRF of IR Materials

The standard MR fluid composition is effective for finishing optical glasses, glass–ceramics, plastics, and some non-magnetic metals.<sup>11</sup> This standard fluid does not perform well on magnetic or IR materials. In this section, we identify IR materials of interest, illustrate some of the difficulties encountered when polishing these materials with the standard MR fluid, and show how new MR fluids and modified processing conditions enable the MRF of IR materials to be accomplished.

### 1. IR Materials of Interest

Some physical properties of eight IR materials of interest to the COM and its collaborators are given in Table 72.V. Properties of BK7 are included for comparison. Data are rank ordered according to increasing hardness. Most of these materials are considerably softer than optical glasses. One is water soluble; two are significantly harder than any glasses. Several of the single-crystal materials exhibit orientational anisotropies in hardness. The two polycrystalline compounds ZnSe and ZnS differ in grain size by an order of magnitude. Samples of most materials listed in Table 72.V were obtained in the form of plugs, 25 to 40 mm in diameter, and subsequently processed on one side into 70-mm-radius spheres. Sapphire samples were provided as bend bars, and the CVD diamond part was in the form of a 1.1-mm-thick by 17-mm-diam disk.

### 2. Processing Limitations of Standard MR Fluid

Table 72.VI gives removal rates and smoothing data for several IR materials under conditions similar, but not identical, to those set forth in Table 72.IV. The modified process conditions (2× lower trough velocity and 50% larger gap—e.g., smaller spot—between workpiece and trough) reduce the polishing efficiency for the BK7 reference part by ~3×, without affecting achievable surface finish. Under these somewhat relaxed conditions, MRF of soft IR materials is too aggressive. Initially smooth surfaces become rougher by anywhere from 2× to 30× after 1-μm-removal runs, and pits and/or scratches appear. Figure 72.33 shows the degradation created in a pitch-polished ZnS surface by MRF.

Conversely, the standard MR fluid has little effect on hard IR materials. The removal rate for sapphire is very small, and no effect is seen for CVD diamond. The correlation between removal rate and material mechanical properties (not shown) is not observed.

### 3. Improved MR Fluids and Process Conditions

Two strategies are found in the literature<sup>27</sup> for polishing IR materials conventionally. One approach uses aqueous-based

Table 72.V: IR material properties.

Material	Source	Structure <sup>(a)</sup>	Water Solubility g/100 g @ 20°C	Knoop Hardness $H_k^{(b)}$ (GPa)	Young's Modulus <sup>23</sup> $E$ (GPa)	Fracture Toughness $K_{Ic}$ (MPa $\cdot\sqrt{m}$ )
LiF	Optovac	cubic sc	0.27 <sup>14</sup>	0.85–0.95 <sup>15</sup>	91	0.36 <sup>(c)</sup>
ZnSe	II–VI	cubic pc, ~50 to 80 $\mu\text{m}$	insoluble	1.08 <sup>16</sup>	67 <sup>16</sup>	0.5 <sup>16</sup>
CaF <sub>2</sub>	Optovac	cubic sc	0.0017 <sup>14</sup>	1.54–1.75 <sup>15</sup>	110	0.33 <sup>(c)</sup>
AMTIR-1	Amorphous materials	glass, Ge <sub>33</sub> As <sub>12</sub> Se <sub>55</sub>	insoluble	1.67 <sup>17</sup>	22 <sup>17</sup>	0.34 <sup>(d)</sup>
ZnS	II–VI, Morton	cubic pc, 2 to 8 $\mu\text{m}$	insoluble	2.11 <sup>16</sup>	75 <sup>16</sup>	0.8 <sup>16</sup>
MgF <sub>2</sub>	Optovac	tetrag. sc, c-cut	insoluble <sup>14</sup>	2.87–4.07 <sup>18</sup>	138	0.9 <sup>(c)</sup>
BK7	Schott, Ohara	glass	insoluble	5.84 <sup>19</sup>	81 <sup>19</sup>	0.85 <sup>20</sup>
Al <sub>2</sub> O <sub>3</sub>	U.S. Army	hexag. sc, c-cut	insoluble	13–21 <sup>21</sup>	405	2.2 <sup>(c)</sup>
CVD diamond	NAWC	cubic pc	insoluble	56–102 <sup>22</sup>	1100 <sup>24</sup>	5–6 <sup>25</sup>

(a)sc = single crystal; pc = polycrystalline (c)Weakest plane

(b)100 gf

(d)Unpublished, measured at COM

Table 72.VI: Removal-rate and smoothing results with standard MR fluid on pitch-polished IR materials.

Conditions:			
<ul style="list-style-type: none"> <li>• Plano-convex plugs, ~25- to 40-mm-diam <math>\times</math> 70-mm radius</li> <li>• Horizontal-trough machine</li> <li>• Trough velocity, 10 rpm (~0.25 m/s)</li> <li>• Work spindle fixed for spots, 38 rpm for polishing</li> <li>• Ribbon height/gap, 2/1.5 mm</li> <li>• Magnet current, 8 A</li> </ul>			
Material	Peak $r$ rate ( $\mu\text{m}/\text{min}$ )	Volume $r$ rate ( $\text{mm}^3/\text{min}$ )	Roughness <sup>26</sup> initial $\rightarrow$ final 1 $\mu\text{m}$ removed rms (nm)
LiF	1.04	0.041	3 $\rightarrow$ 5 (p) <sup>(a)</sup>
ZnSe	0.34	0.012	4 $\rightarrow$ 75 (p, scr)
CaF <sub>2</sub>	0.26	0.029	2 $\rightarrow$ 16 (p)
AMTIR-1	4.21	0.36	2 $\rightarrow$ 4 (scr)
ZnS	0.17	0.006	4 $\rightarrow$ 132 (p)
MgF <sub>2</sub>	0.17	0.017	2 $\rightarrow$ 10 (p, scr)
BK7	1.78	0.18	1 $\rightarrow$ 1
Al <sub>2</sub> O <sub>3</sub>	0.036	0.002 <sup>(b)</sup>	na
CVD diamond	na	na	na

(a)p = pits; scr = scratches.

(b)Trough velocity, 20 rpm; spindle velocity, 75 rpm.

slurries containing alumina (coarse/ $0.3\ \mu\text{m}$  to fine/ $0.05\ \mu\text{m}$ ) on a pitch or wax lap at low (50-gf) loads.<sup>27,28</sup> Another approach recommends diamonds (coarse/ $3.0\ \mu\text{m}$  to fine/ $1.0\ \mu\text{m}$ ) in nonaqueous (or partially aqueous) glycol-based suspensions.<sup>29</sup> It is recommended that, in order to prevent pits or scratches, removal rates should be low in the final finishing stages for soft materials.

Alumina or diamond abrasives are easily substituted for  $\text{CeO}_2$  in the MR fluid. Table 72.VII gives the properties of some submicron-size alumina and diamond polishing agents used in this work. Two interesting materials are the

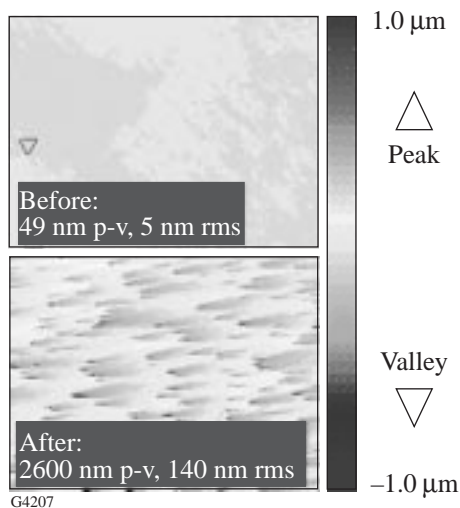


Figure 72.33  
2.6- $\mu\text{m}$ -deep pits on a 0.25-mm  $\times$  0.35-mm area of ZnS after removing 1  $\mu\text{m}$  of material with MRF under conditions in Table 72.VI.<sup>26</sup>

“nanoalumina” and “nanodiamond” products, which are in the 0.04- $\mu\text{m}$  size range. Figure 72.34 gives a nomograph showing, for a given particle size (assumed monosized), how many particles would be contained in 1 ml of MR fluid prepared from a given volume percent of abrasive. The standard MR fluid has  $\sim 10^9$   $\text{CeO}_2$  particles per milliliter. There are nearly  $10^{14}$  nanoabrasive particles dispersed in the MR fluid when it is prepared with as little as 0.1 vol % of these materials.

a. Removal rates with alumina-based MR fluids. The MR fluid is adjusted for IR materials by substituting 0.3  $\mu\text{m}$  alumina at  $\sim 5$  vol % for  $\text{CeO}_2$ , and by further relaxing process

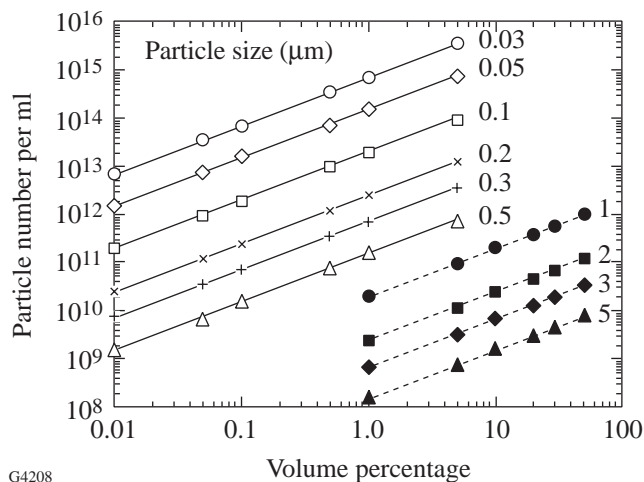


Figure 72.34  
Nomograph for estimating the number of abrasive particles in 1 ml of MR fluid, based upon volume percent and particle size (assumed monosized).

Table 72.VII: Polishing abrasives for IR materials.

Abrasive	Source <sup>30</sup>	Structure	Form of Supply	Particle size <sup>(a)</sup> ( $\mu\text{m}$ )	
				Primary <sup>(b)</sup>	Aggregate/Agglomerate
9220 nanoalumina	Norton Co.	alpha platey	19%–23% solids	0.04	0.07/—
“B” alumina	Praxair	gamma blocky	dry	0.09	0.16/—
“A” alumina	Praxair	alpha platey	dry	$\sim 0.3$ <sup>(c)</sup>	na
DIANAN <sup>®</sup> nanodiamonds	Mark Technologies	—	dry	0.03	—/0.75

(a) Numerical average of 20 primary particles by JEOL 200 EX transmission electron microscopy (TEM).

(b) *Primary particles*: single domain, homogeneously ordered, single crystals; *aggregates*: strongly bonded assembly of two or more primary particles; *agglomerates*: weakly bonded ensemble of primary particles, aggregates, or both.<sup>31</sup>

(c) From vendor literature.

polishing aggressiveness with reductions to trough velocity, gap, and magnet current. As shown in Table 72.VIII, volumetric removal rates for the BK7 reference are now 22× and 60× lower than those reported, respectively, in Tables 72.VI and 72.IV. Volumetric removal rates for the IR materials (Table 72.VIII compared to Table 72.VI) have actually increased (LiF, +3×; ZnSe, +1.3×), remained approximately the same (CaF<sub>2</sub>, ZnS), or dropped (AMTIR-1, -3×; MgF<sub>2</sub>, -8.5×). Figure 72.35 shows that the correlation previously established between removal rates and mechanical properties for MRF of glasses with CeO<sub>2</sub> in the MR fluid is preserved for alumina slurries, and it is now seen to hold for IR materials as well. The advantage to these adjustments is smoothing without scratching or pitting for IR materials.

Table 72.VIII: Removal-rate results for IR materials with alumina-based MR fluids and relaxed process conditions.

Conditions:		
<ul style="list-style-type: none"> <li>• Plano-convex plugs, ~25- to 40-mm-diam × 70-mm radius, pitch polished</li> <li>• Horizontal-trough machine</li> <li>• 0.3-μm alumina abrasive in MR fluid</li> <li>• Trough velocity, 5 rpm (~0.13 m/s)</li> <li>• Work spindle, fixed (spots)</li> <li>• Ribbon height/gap, 1.5 to 2/1 to 1.5 mm</li> <li>• Magnet current, 1 A</li> </ul>		
Material	Peak <i>r</i> rate (μm/min)	Volume <i>r</i> rate (mm <sup>3</sup> /min)
LiF	4.07	0.149
ZnSe	0.57	0.016
CaF <sub>2</sub>	0.40	0.024
AMTIR-1	3.68	0.127
ZnS	0.22	0.007
MgF <sub>2</sub>	0.21	0.002
BK7	0.35	0.008
SF7	0.51	0.013
FS	0.16	0.005

b. IR material finishing experiments with modified MR fluids. Details of finishing experiments for IR materials with alumina- and diamond-based MR fluids are given in Table 72.IX. Indicated across the top and down the left-hand side of the table are the machine processing conditions and abrasives used for each material. The middle of the table gives results of smoothing experiments conducted on ring-tool-

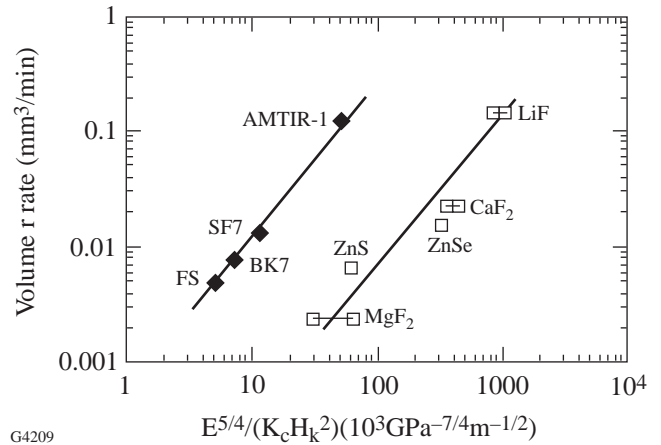


Figure 72.35: Volumetric removal rates for IR materials and optical glasses using an alumina-based MR fluid, plotted against mechanical properties.

generated parts,<sup>32</sup> and results from figure-correction experiments are summarized on the right-hand side of the table.

Surface smoothing without the generation of pits or scratches is seen for all materials. Roughness in LiF, CaF<sub>2</sub>, AMTIR-1, ZnS, and MgF<sub>2</sub> is reduced from ~2000 nm to 4 to 6 nm with alumina abrasives under relaxed MRF conditions. Examples of smoothing are given for AMTIR-1 and ZnS in Fig. 72.36.

The addition of as little as 0.14-vol % nanodiamonds to the standard MR fluid significantly improves removal rates for sapphire, as was previously reported.<sup>33</sup> Table 72.IX (bottom) shows the results of an experiment to process four bend bars (3 mm × 4 mm × 45 mm long) meant for fracture strength testing.<sup>34</sup> Work was conducted with the vertical-wheel machine, using translational motion of the part along the fluid ribbon without spindle rotation. MRF reduces p-v and rms roughness of initially ground surfaces by ~10× after 4 to 6 h. Simultaneously, because of the compliant nature of the spot and its large lateral size relative to the part width, the sharp edges of the part adjacent to the work surface are smoothed. Figure 72.37 shows the setup, a part, and part edges before and after MRF. Most edge chips, cracks, and scratches are removed.

An MR fluid with 0.14-vol % nanodiamonds can be used for room-temperature polishing of CVD diamond. Table 72.IX shows that, in 80 h of elapsed polishing time, MRF with the vertical-wheel machine reduces the p-v roughness of CVD diamond from almost 9 μm to under 1 μm. The rms roughness is reduced by 10× to under 40 nm.

Table 72.IX: Finishing results for IR materials with alumina- or diamond-based MR fluids and relaxed process conditions.

Conditions:					Smoothing		Finishing	
Material	Abrasive/ vol %	Trough Vel./ Spindle Vel. (rpm)	Ribbon ht/ gap ht (mm)	Amount Material Removed ( $\mu\text{m}$ )	Roughness initial→final	Roughness initial→final	Fig. Error <sup>10</sup> initial→final (90% aperture) ( $\mu\text{m}$ )	Amount Material Removed ( $\mu\text{m}$ )
					p-v ( $\text{nm}^{26}$ )	rms ( $\text{nm}^{26}$ )		
LiF	B alumina/2.7	10/53	1.5/1	3	1880→45	50→3		
ZnSe	9220 nano/5.4	20/75	2/1	20	2000→250	180→15		
CaF <sub>2</sub>	A alumina/5.1	15/53	2/1.5	3	650→35	12→4	0.63→0.16 0.63→0.32	0.65 1.0
AMTIR-1	B alumina/2.7	1.9/53	2/1.5	9	2370 <sup>(b)</sup> →30	100→4		
ZnS	A alumina/5.1	20/75	2/1.5	9	2550→56	108→6	0.63→0.16	0.3
MgF <sub>2</sub>	B alumina/2.7	20/75	2/1	9	2340→50	57→6	0.19→0.63	1.0
BK7	A alumina/5.1	15/53	2/1.5	6	2410→20	73→1	0.32→0.13	1.0
Al <sub>2</sub> O <sub>3</sub>	CeO <sub>2</sub> Std <sup>(a)</sup> /5.7	175/none	2/1	na	8650→1365	540→56		
CVD diamond	9220 nano <sup>(a)</sup> /2.5	175/100	2/1	11	8735→840	435→39		

(a)With 0.14-vol % DIANAN<sup>®</sup> nanodiamonds.

(b)Initial surface, loose abrasive ground with 3- $\mu\text{m}$  alumina.

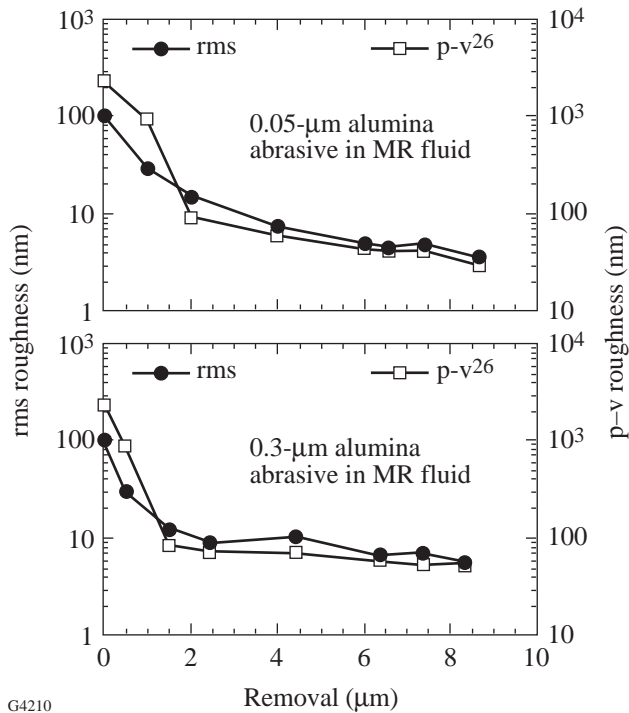


Figure 72.36

(a) Smoothing of AMTIR-1 with MRF after grinding with 3- $\mu\text{m}$  loose abrasives; (b) smoothing of ZnS with MRF after grinding with 2- to 4- $\mu\text{m}$  fine diamond ring tool on a Rogers & Clarke GP 150.

Two types of artifacts from the MRF smoothing process require further study. One type of artifact is seen in the processing of curved surfaces on single-crystal CaF<sub>2</sub> and MgF<sub>2</sub>. For small amounts of material removed (e.g., 0.5  $\mu\text{m}$ ) during figure-correction runs, surface figure errors are corrected well. In removing larger amounts of material (e.g., >1  $\mu\text{m}$ ), asymmetric features are seen to develop that may relate to orientational anisotropies in mechanical properties for these crystals.<sup>15,18</sup> An example for CaF<sub>2</sub> is shown in Fig. 72.38. Similar behavior in MgF<sub>2</sub> causes the increase in figure error reported in Table 72.IX.

A second type of artifact is seen in finishing ZnSe. As shown by the smoothing data in Table 72.IX, gross roughness is reduced by MRF, but only to a level that is ~10 $\times$  higher than that achieved for other crystals. Microscopic examination shows that the surface features causing this microroughness are not pits or scratches but are a manifestation of hills and valleys on the part surface whose lateral feature size is comparable to the ZnSe grain size (see Fig. 72.39).<sup>26</sup> The irregular surface texture is called “orange peel” and is related to the chemistry and mechanics of the polishing process.<sup>35</sup> More work is required to adjust the MRF process for finishing ZnSe.



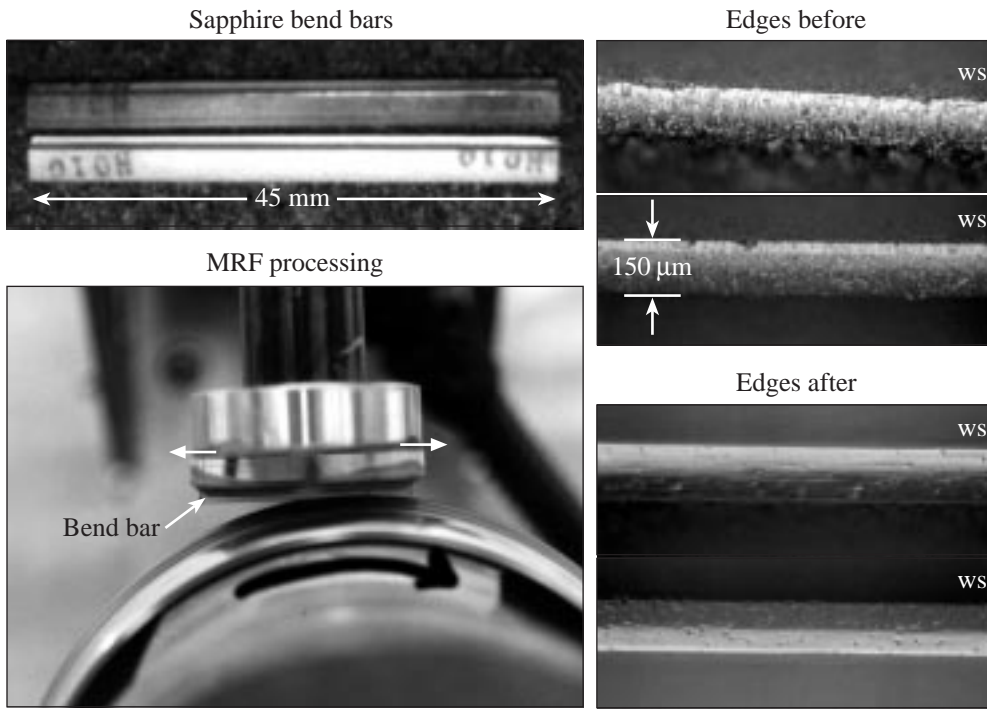
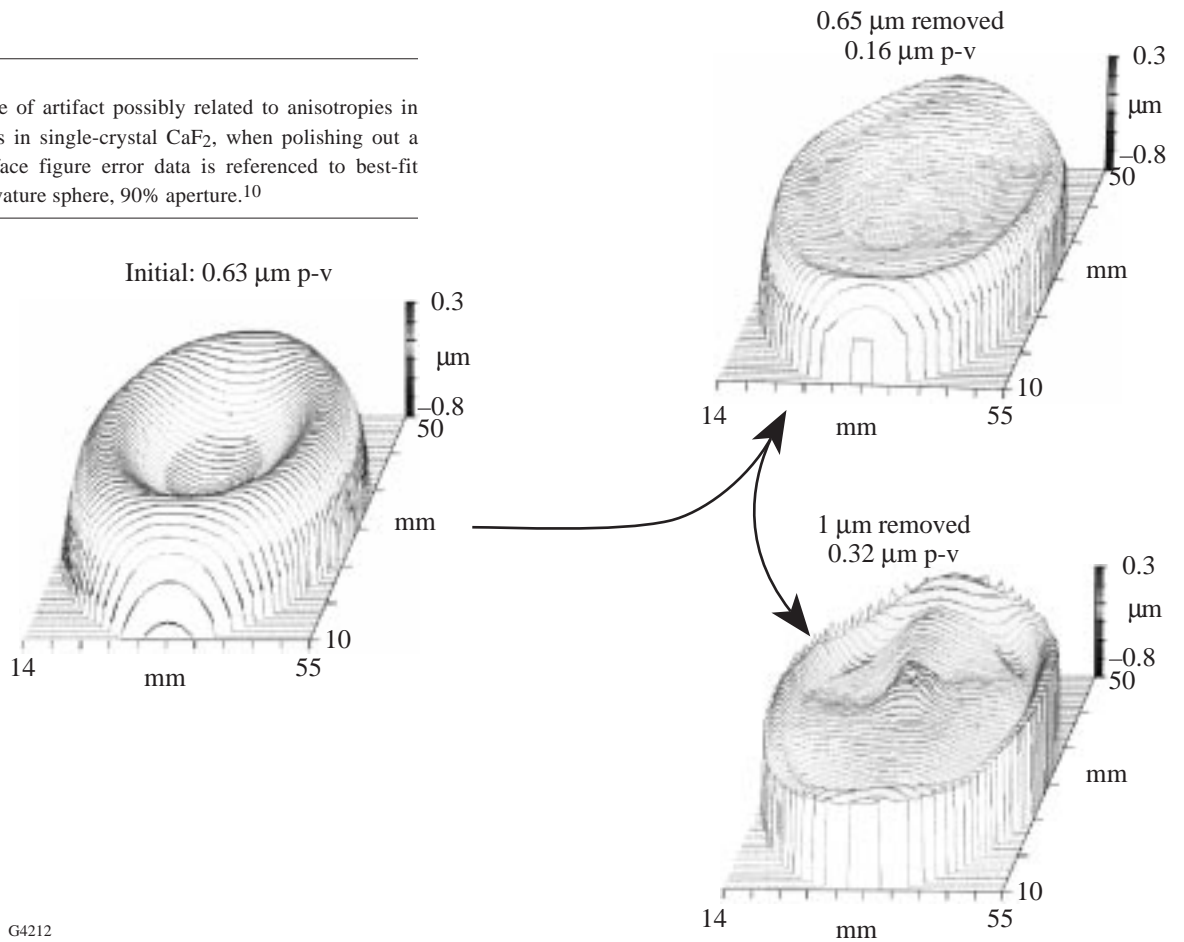


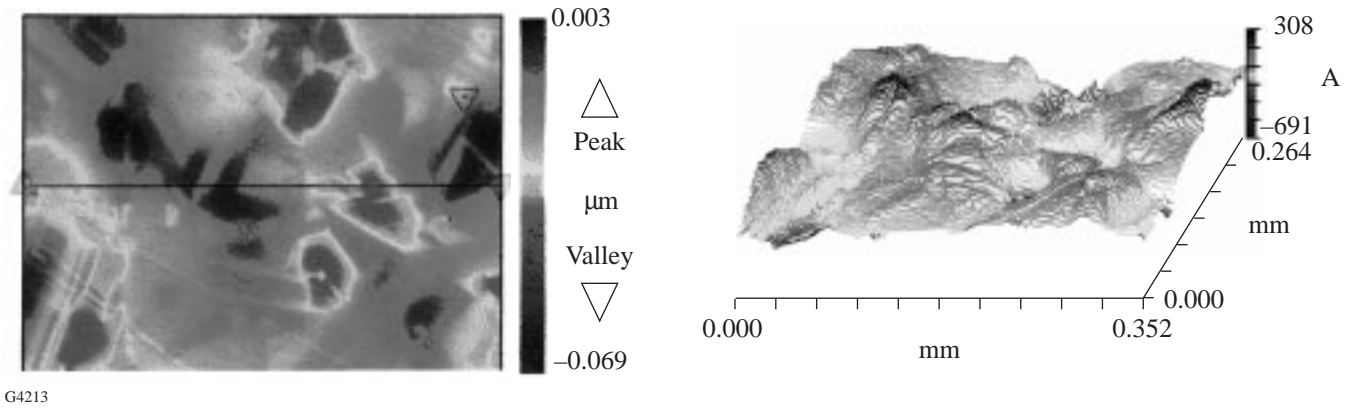
Figure 72.37  
MRF processing of sapphire bend bars by the translation along the ribbon. The nanodiamond doped MR fluid removes edge chips, cracks, and scratches (ws = work surface).

G4211

Figure 72.38  
Evolution of one type of artifact possibly related to anisotropies in mechanical properties in single-crystal CaF<sub>2</sub>, when polishing out a convex surface. Surface figure error data is referenced to best-fit 70-mm radius-of-curvature sphere, 90% aperture.<sup>10</sup>



G4212



G4213

Figure 72.39  
Characteristic texture called “orange peel” in the surface of a ZnSe part after MRF.

4. Aspheric Surface on AMTIR-1

An important goal of MRF is the ability to finish aspheric lens surfaces for use in IR imaging systems. This article concludes with an example of rapid aspheric surface manufacturing using the IR material AMTIR-1.

A 40-mm-diam by 8-mm-thick part was cut to a base radius of 70 mm with a series of three bronze-bonded, diamond ring grinding tools on the Optipro® SX50.<sup>36</sup> The part was prepolished for

10 min on a special lap<sup>37</sup> to remove deep tool marks. This surface was then processed by MRF in three runs (~24 min) to remove surface microroughness and change the surface from a sphere to an asphere with a conic constant of -0.35 (ellipse). Processing conditions and results are given in Table 72.X. A nanoalumina polishing agent was used in the MR fluid. Figure 72.40 gives the required radial deviation from least-removal sphere<sup>38</sup> and stylus profiler scans<sup>39</sup> of the part surface before/after MRF processing. The final figure was 0.13 μm.

Table 72.X: MRF results for AMTIR-1 ellipse.

Conditions:				
<ul style="list-style-type: none"> <li>• Plano-convex plug, 40-mm diam × 70-mm radius</li> <li>• MR fluid, 2.4-vol % 9220 nanoalumina</li> <li>• Vertical-wheel machine</li> <li>• Wheel velocity, 175 rpm (~1.4m/s)</li> <li>• Work spindle velocity, 55 rpm</li> <li>• Ribbon height/gap, 2/1 mm</li> <li>• Magnet current, 2.5 A</li> </ul>				
Process Step (time, min)	Amount Material Removed (μm)	Final Roughness p-v (nm <sup>26</sup> )	Final Roughness rms (nm <sup>26</sup> )	Final Figure <sup>(a)</sup> Error p-v (μm)
Grind	—	2510	194	—
Prepolish (10)	—	300	5	5.11
Run #1 (14)	4	15	2	0.79
Run #2 (7)	1	13	1.5	0.20
Run #3 (2.5)	0.5	13	1.4	0.13

<sup>(a)</sup>Ref: least-removed sphere.

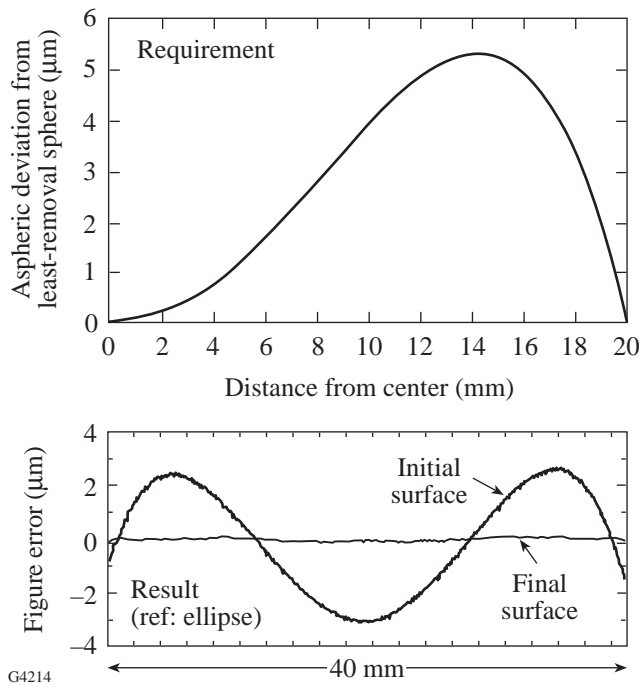


Figure 72.40  
Aspheric finishing of AMTIR-1 part.

## Conclusion

MRF of optical glasses is accomplished with an MR fluid containing  $\text{CeO}_2$  to accelerate removal rates. By substituting nanoalumina or nanodiamond abrasives for  $\text{CeO}_2$  and making changes to the MRF process conditions, it is possible to finish IR materials as well. Work will continue to understand process chemistry and the mechanics of removal for these materials to further improve the quality of finish.

## ACKNOWLEDGMENT

The following companies, laboratories, and agencies are acknowledged for providing material: Optovac, II-VI, Inc.; Morton International Advanced Materials, Inc.; Lockheed Martin; the U. S. Army; the Naval Air Warfare Center; Ohara Corp.; Hoya Corp. USA; Schott Glass Technologies; Heraeus Amersil, Inc.; and Corning, Inc., Advanced Materials. D. Rostoker supplied information on the chemistry of nanoalumina suspensions. Support for this work is provided by Byelocorp Scientific, Inc., the U.S. Army Materiel Command, and the Defense Advanced Research Projects Agency (DARPA).

## REFERENCES

1. W. I. Kordonski and S. D. Jacobs, *Int. J. Mod. Phys. B* **10**, 2837 (1996).
2. D. Golini, S. Jacobs, W. Kordonski, and P. Dumas, in *Advanced Materials for Optics and Precision Structures*, edited by M. A. Ealey, R. A. Paquin, and T. B. Parsonage, *Critical Reviews of Optical Science and Technology* (SPIE, Bellingham, WA, 1997), Vol. CR67, pp. 251–274.

3. T-bar spindle @ 8/s on a Brookfield RVTDV-II Digital Viscometer, Brookfield Engineering Laboratories, Stoughton, MA 02072.
4. A. Shorey, unpublished data (June 1997).
5. Horiba LA900 Particle Size Analyzer, Horiba Instruments Inc., Irvine, CA 92714.
6. EW grade, BASF Corp., Mount Olive, NJ 07828.
7. CeRite 4250, dry, 50%  $\text{CeO}_2$  with other rare earths, Ferro Corp., Transelco Division, Penn Yan, NY 14527.
8. S. D. Jacobs, D. Golini, Y. Hsu, B. E. Puchebner, D. Strafford, Wm. I. Kordonski, I. V. Prokhorov, E. Fess, D. Pietrowski, and V. W. Kordonski, in *Optical Fabrication and Testing*, edited by T. Kasai (SPIE, Bellingham, WA, 1995), Vol. 2576, pp. 372–382.
9. W. I. Kordonski, S. D. Jacobs, D. Golini, E. Fess, D. Strafford, J. Ruckman, and M. Bechtold, in *Optical Fabrication and Testing*, 1996 Technical Digest Series (Optical Society of America, Washington, DC, 1996), Vol. 7, pp. 146–149.
10. Zygo Mark IVxp, Zygo Corp., Middlefield, CT 06455.
11. J. Lambropoulos, F. Yang, and S. D. Jacobs, in *Optical Fabrication and Testing*, 1996 Technical Digest Series (Optical Society of America, Washington, DC, 1996), Vol. 7, pp. 150–153.
12. Zygo Maxim 3D, Zygo Corp., Middlefield, CT 06455.
13. Chapman MP 2000, Chapman Instruments, Rochester, NY 14623.
14. Data from *BDH CRYSTRAN Product Handbook* (BDH Ltd., Poole, England, 1990).
15. C. A. Brookes, J. B. O'Neill, and B. A. W. Redfern, *Proc. R. Soc. Lond. A* **322**, 73 (1971).
16. Product brochure(s) from Morton International Advanced Materials, Woburn, MA 01801-6278 (1995); II-VI Inc., Saxonburg, PA 16056 (1991).
17. Product brochure(s) from Amorphous Materials, Inc., Garland, TX 75042 (1996).
18. N. D. Zverev *et al.*, *Sov. J. Opt. Technol.* **58**, 361 (1991).
19. Hoya Optical Glass Catalog (1985).
20. J. C. Lambropoulos, S. Xu, and T. Fang, *Appl. Opt.* **36**, 1501 (1997).
21. B. G. Pazol *et al.*, in *Window and Dome Technologies and Materials III*, edited by P. Klocek (SPIE, Bellingham, WA, 1992), Vol. 1760, pp. 55–65.
22. H. O. Pierson, *Handbook of Carbon, Graphite, Diamond, and Fullerenes: Properties, Processing, and Applications* (Noyes Publications, Park Ridge, NJ, 1993).
23. Except where indicated, data is from W. F. Krupke *et al.*, *J. Opt. Soc. Am. B* **3**, 102 (1986).

24. W. Banholzer, T. Anthony, and R. Gilmore, in *New Diamond Science and Technology*, 1991 MRS Int. Conf. Proc. (Materials Research Society, Pittsburgh, 1993), pp. 857–862.
25. M. D. Drory *et al.*, *J. Appl. Phys.* **78**, 3083 (1995).
26. Areal, 0.25 mm × 0.35 mm, 20x Mirau, Zygo NewView® 100, Zygo Corp., Middlefield, CT 06455.
27. G. W. Fynn and W. J. A. Powell, *Cutting and Polishing Optical and Electronic Materials*, 2nd ed., The Adam Hilger Series on Optics and Optoelectronics, edited by E. R. Pike and W. T. Welford (A. Hilger, Bristol, 1988), pp. 215–220.
28. Kodak Publication U-72, Kodak Intran Infrared Optical Materials (1971), as cited in A. S. De Vany, *Master Optical Techniques*, Wiley Series in Pure and Applied Optics (Wiley, New York, 1981), p. 235; or as cited in D. F. Horne, *Optical Production Technology*, 2nd ed. (Hilger, London, 1972), p. 252.
29. For example, Engis Hyprez Hyprelube® (polyalkylene glycol), and W Lubricant (polyglycol ether).
30. 9220 nanoalumina from Norton Company, Worcester, MA; Praxair “B” and “A” aluminas [equivalent to Linde “B” and “A”] from Universal Photonics, Inc., Hicksville, NY; DIANAN® nanodiamonds from Mark Technologies International, LLC (Strauss Chemical Co.), Elk Grove, IL.
31. *Fundamentals of Particle Sizing*, Nanophase Technologies Corp., Burr Ridge, IL 60521 (1994).
32. D. Golini and W. Czajkowski, *Laser Focus World*, July 1992, 146.
33. S. D. Jacobs, *Finer Points* **7**, 47 (1995).
34. Sapphire Statistical Characterization and Risk Reduction (SSCARR) Program, BMDO/AQS Quarterly Review, Nichols Research Corp., Hunstville, AL (12 March 1997).
35. A discussion of “orange peel,” haze, pits, and scratches, and how they are affected by slurry chemistry and polishing conditions for pad polishing, is given in H. Matsushita, M. Ishida, and J. Kikawa, *J. Cryst. Growth* **103**, 448 (1990).
36. OptiPro Systems, Inc., Ontario, NY 14519.
37. D. A. VanGee (private communication).
38. The least-removed sphere is the sphere that passes through the center and edge of an asphere. It does not necessarily represent the best-fit sphere.
39. Form Talysurf®, Taylor Hobson, Leicester, UK.